Magnetotransport and Trapping of Magnetic Domain Walls in Spin Valves With Nanoconstrictions

S. J. Noh[1], B. S. Chun[1], H. C. Wu[2], I. V. Shvets[2], I. C. Chu[3], M. Abid[4], S. Serrano-Guisan[5], and Y. K. Kim[1]

[1]Department of Materials Science and Engineering, Korea University, Seoul 136-713, Korea
[2]CRANN,School of Physics, Trinity College Dublin, Dublin 2, Ireland
[3]Data and Storage R&D Laboratory, LG Electronics, Seoul, 153-801, Korea
[4]Ecole Polytechnique Federale de Lausanne/IPMC, Lausanne 1015, Switzerland
[5]Physikalisch-Technische Bundesanstalt, Braunschweig 38116, Germany

In a magnetic nanowire, a magnetic domain wall (DW) can move along the wire when an applied magnetic field or a spin-polarized current is applied. A magnetic spin-valve device composed of two nanowires connected by a nanosized constriction was prepared, on which the presence of a pinned DW by nanoconstriction was detected by giant magnetoresistance effect. When the magnetic wire has a nanoconstriction, the DW configuration and width were largely affected by the shape of nanoconstriction. An asymmetric magneto-transport behavior observed in the experiments was interpreted by a micromagnetic modeling study.

Index Terms—**Nanoconstriction, nanowire, magnetic domain wall (DW), magnetoresistance.**

I. Introduction

DOMAIN WALL (DW) and its motion in magnetic nanowires and stripes have attracted a large amount of attention in terms of understanding fundamental physics as well as for potential technological applications [1]–[3]. The latter has been recently demonstrated for logic and memory devices [1], [2].

Generally, the magnetization in a ferromagnetic nanowire tends to lie parallel to the wire axis due to shape anisotropy. In such a nanostructure, it is now well established that a magnetic field or an electrical current can drive the DW motion. In the case of the electrical current, the DW motion occurs via a coupling between conduction electrons and local magnetic moments [4], [5]. In general, the mechanism underlying the DW propagation follows two steps, namely, the DW nucleation and DW propagation. In addition, the DW nucleation can be induced with a local magnetic field generated by an overlying current through the wire. The head-to-head and tail-to-tail DWs can be defined in this way by charging the polarity of the current in the current carrying wire.

Nowadays, it is still a great challenge to control the DW position for the development of reproducible and reliable magnetic devices using the current-induced DW motion. One of the most promising DW control methods is to place notches on the magnetic nanowire. In this case, the DWs are pinned at the notches due to a lower energy state [6]. Another less explored method was proposed by Bruno [7], consisting of a nanoconstriction, where a DW wall is geometrically constrained. A typical magnetic nanoconstriction system can be composed of two wires with different widths connected by a nanosized constriction. Moreover, Kim *et al.* [8], based on the micromagnetic modeling, shows that the nanoconstriction shape is a key parameter to determine DW configuration and DW width. It is well known that the presence of a pinned DW in such nanostructure can be probed easily by measuring the giant magnetoresistance (GMR) effect which is sensitive to the relative magnetization orientations of the two wires. Apart from the DW and DW motion area in the field of spintronics, spin valves (SVs) are still an active field of research. Therefore, further understanding of the magneto-transport properties in SVs with nanoconstrictions is of high importance.

Here, we investigate the effect of the nanoconstriction shape on the DW pinning and depinning by using an SV structure in current-in-plane (CIP) configuration. Our results show an asymmetric magnetotransport curve which depends on the applied magnetic field direction with respect to the nanoconstriction shape.

II. Experimental Procedure

Samples used for this investigation were of the following stacks; Si/SiO_2/Ta 5/NiFe 3.5/CoFe 5/Cu 2.8/CoFe 3.5/IrMn 10/Ta 5 (in nm). Samples were prepared using a six-target dc magnetron sputtering system under the typical base pressure of less than 2×10^{-7} Torr. The easy axes of the magnetic layers were aligned along the same direction by applying 100 Oe of magnetic field during deposition. The magnetoresistance of the constricted SV structure was characterized by a probe station with an external magnetic field of up to 1400 Oe. All microstructures discussed in this paper were fabricated from the same SV thin film. Device fabrication was carried out by e-beam lithography using a negative tone ma-N 2403 resist and Ar^+ ion etching. Subsequently, after removal of the resist, UV lithography pattern has been carried out to fabricate the macroscopic metal contacts. The metal contacts consist of 35-nm-thick Au, and 5 nm of Ti which serves as an adhesive layer. In order to interpret the experimental data, we have employed micromagnetic computation based on the Landau–Lifschitz–Gilbert (LLG) equation.

Manuscript received February 21, 2011; revised April 26, 2011; accepted May 23, 2011. Date of current version September 23, 2011. Corresponding author: Y. K. Kim (e-mail: ykim97@korea.ac.kr).

Color versions of one or more of the figures in this paper are available online at http://ieeexplore.ieee.org.

Digital Object Identifier 10.1109/TMAG.2011.2158400

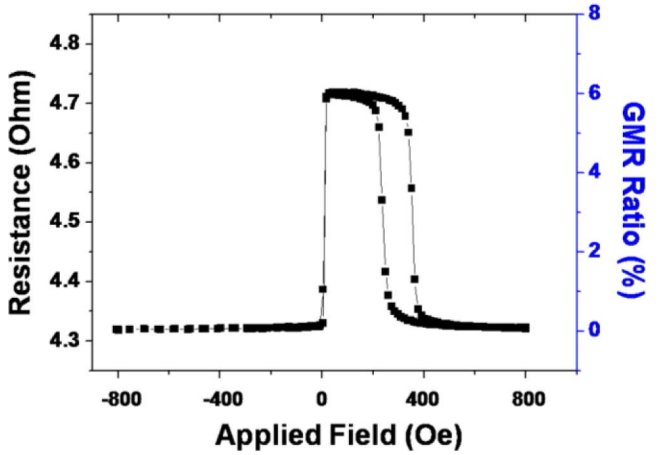

Fig. 1. Magneto-transport properties of an unpatterned Ta 5/NiFe 3.5/CoFe 5/Cu 2.8/CoFe 3.5/IrMn 10/Ta 5 (nm) SV sample.

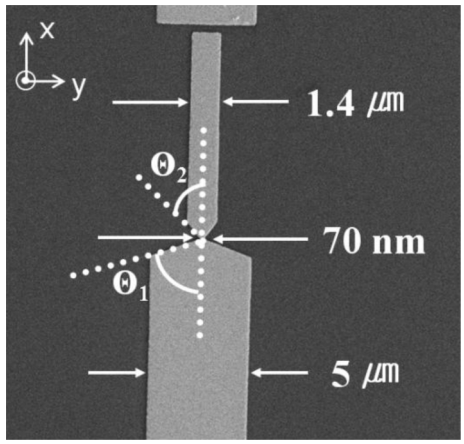

Fig. 2. SEM image of a patterned device. Pads with different sizes were designed to induce different switching fields resulting from the difference in shape anisotropy.

III. Results and Discussion

Before implementing the nanoconstricted SV structure, we have fully characterized the exchange coupling strength and the magnetoresistance of the multilayered SV. The SV structure was designed with a quasi zero magnetostatic coupling between the pinned and free layer across the nonmagnetic Cu spacer. Moreover, we optimized the multilayered stack by changing the layer thicknesses in order to fulfill two objectives: first, a good exchange coupling strength, and, second, a good magnetoresistance ratio for the CIP configuration.

Fig. 1 shows a typical magneto-transport curve of an unpatterned SV. During the measurement, the magnetic field was applied parallel to the magnetic easy axis of the free and pinned layers. This SV exhibits a GMR of 6% with an exchange coupling strength of 350 Oe. This magnetoresistance corresponds to a sensitivity (an average slope during the free-layer magnetization switching defined as, $S\,(\%/\mathrm{Oe}) = \mathrm{GMR}/\Delta H$) of 0.5%/Oe in the center of the ascending branch. This SV also exhibits an interlayer exchange coupling field of 10 Oe.

A scanning electron microscope (SEM) image of the patterned SV device is depicted in Fig. 2. In order to trap a DW, we have patterned a nanoconstriction into the SV wire. The V-shaped nanoconstriction with a size of 70 nm is located in the middle of two pads with different widths. These pads act as reservoirs where DWs are injected toward the nanoconstriction. These reservoirs are designed to introduce a different switching field due to the shape anisotropy. The shape anisotropy of the wire constrained the magnetizations of both pinned and free layers to align parallel to the wire axis.

Fig. 3 displays the magnetotransport data of the patterned SV with a nanoconstriction where the film structure is the same as the one shown in Fig. 1. Theses curves exhibit a typical asymmetric behavior with different polarity. When the field was swept from the negative to positive direction, first all layers were aligned parallel to the field direction (lowest resistance state which corresponds to the saturation state). By increasing the field to the positive direction (black curve in Fig. 3), the DW inside the largest reservoir (5-μm width) was nucleated until a head-to-head DW was injected into the free layer of the wire

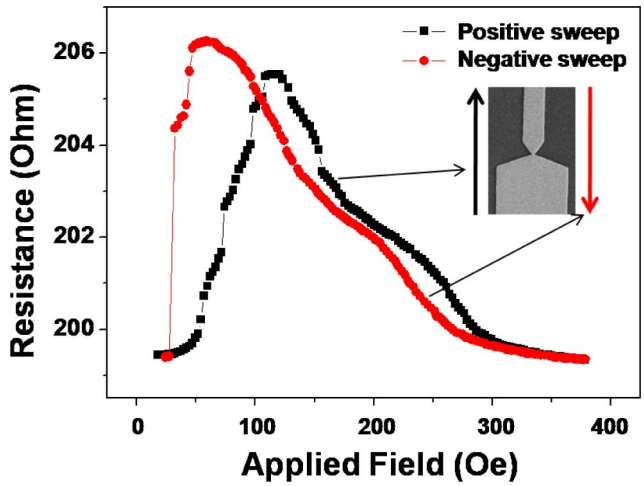

Fig. 3. Magnetotransport properties of the patterned SV structure with a nanoconstriction. The positive sweep (black squared symbol) and negative sweep indicate the direction of the applied magnetic field from thick pad to thin pad (bottom to top in Fig. 2) and vice versa, respectively.

from the reservoir. Second, at 60 Oe, the DW reached the constriction and was trapped. Here, we observe a relatively large shift from the origin (the positive sweep curve in Fig. 3 with black square symbols) in the MR curves in the nanoconstricted SV compared to that of the unpatterned one (in Fig. 1). This shift is mainly due to two effects: first, the magnetostatic coupling between the pinned and free layer or/and, second, the imperfect saturation of the free layer where a few magnetic domains might be present in some portion of the sample but were not detected by the MR measurement [9].

The resistances as a function of applied field curves show many kinks and jumps which are related to the DW in free-layer pinning and depinning at or near the nanoconstriction. In the field of 120 Oe, the magnetization of free layer and pinned layer are completely in antiparallel configuration which leads to the highest resistance state. Further increase of the applied field, a head-to-head DW in the pinned layer was injected to the constriction and, then, trapped in the constriction area. When the applied field became larger than 300 Oe, finally the magnetizations of the free and pinned layers were completely in parallel

configuration (lowest resistance state). After reaching the positive saturation field, the applied field was then swept to the negative direction to nucleate a DW inside the relatively smaller reservoir of 1.4-μm-width pad until a tail-to-tail DW was injected into the wire from the reservoir. In contrast to the positive sweep, when the DW was injected into the wire, less intermediate trapping steps at the nanoconstriction were observed.

According to the micromagnetic modeling study by Kim *et al.* [8], the DW configuration and width appeared were largely affected by the shape of the nanoconstriction (i.e., the angles ($\Theta_{1,2}$) between the *x*-axis and the edge of the wire). To reduce magnetostatic energy, generally the magnetic moments tend to align parallel to the edges. If the angle between the nearest-neighbor spin moments in the constriction becomes smaller (in our case Θ_2, see Fig. 2), the DW width becomes wider. For the larger angle case (in our case, Θ_1), magnetic moments near the constriction align toward the direction perpendicular to the plane, and, as a consequence, the DW width becomes narrower. The DW width becomes wider as the angle of the constriction becomes lower, because the angle between the nearest neighbor spin moments in the constriction becomes small.

As shown in Fig. 2, the 1.4-μm-width reservoir has a large shape anisotropy compared to 5-μm-width one, meaning that the DW injected from the smaller pad is wider, and has less trapping steps which can be understood from the instability of the DW configuration. Therefore, in the constriction between two pads, more complicated pinning process is expected.

In order to interpret the experimental data, we have employed a micromagnetic modeling study based on the LLG equation solver. The dimensions of the calculated nanowire are shown in Fig. 4. Calculation parameters such as saturation magnetization of 1400 emu/cm^3, polarization of 0.4, and exchange stiffness of 1.05 erg/cm were used. The unit vector size was 3.5 nm $\times$ 3.5 nm. The time step was 4.74×10^{-3} ps, and conversion was set at 1×10^{-5} for calculation. The boundary condition used in the calculation was that the magnetization directions of both ends of the wire were fixed to the antiparallel directions (head-to-head DWs). In this figure, the arrow indicates the magnetic moment direction of the unit cell, and the same-colored zone represents the same magnetization direction. Fig. 4(a) and (b) shows the calculated results of the DW instability configuration in the constricted region of the SV corresponding to the kinks and jumps appearing in Fig. 3.

When the field of 1000 Oe was swept from the negative to positive direction, as shown in Fig. 4(a) (related to the positive sweep in Fig. 3) multiple narrow-sized DWs were formed at the nanoconstriction. When the field of 1000 Oe was swept from the positive to negative direction, as in Fig. 4(b) (corresponds to the negative sweep in Fig. 3) less DWs with wider size were formed at the nanoconstriction. When the DW was injected from a small pad, less intermediate trapping steps at the nanoconstriction were observed compared to the DW injected from a large pad.

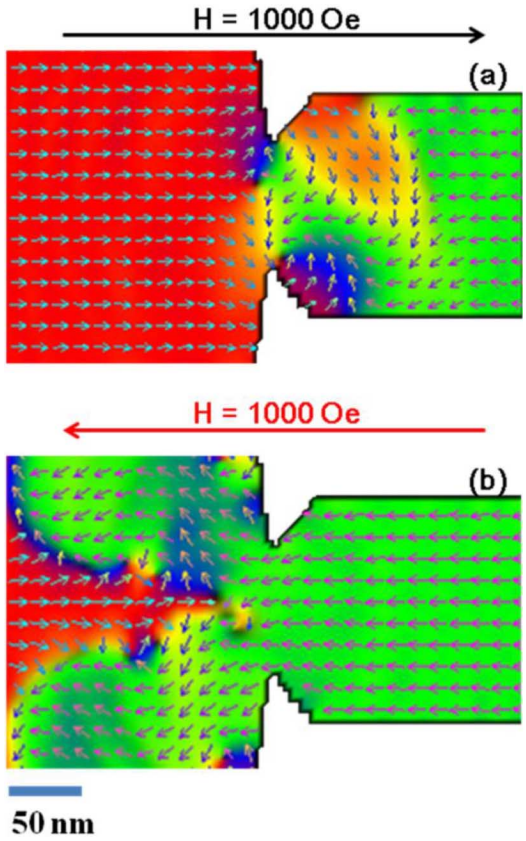

Fig. 4. Calculated results of the DW instability configuration in the constricted region which corresponds to the kinks and jumps appearing in Fig. 3. Arrow indicates the magnetic moment direction in the unit cell, while the same colored zone represents the same magnetization direction. The magnetic fields of $H = 1000$ Oe was swept from the negative to positive direction in (a), and vice versa in (b).

IV. Conclusion

In this study, we investigated the magnetic DW pinning and depinning behaviors using an SV structure with a nanoconstriction. We observed asymmetric magneto-transport curves depending on the direction of the applied magnetic field. An asymmetric magnetotransport behavior was strongly correlated with the shape of the nanoconstriction. When the DW injected from the small pad with small angles between the *x*-axis and the edge of the wire, less intermediate trapping steps at the nanoconstriction are observed compared to the DW injected from large pad with the large angles between the *x*-axis and the edge of the wire. These are resulted from the shape anisotropy difference between the small pad and the large pad. It is emphasized that the nanoconstriction shape determines DW stability, and its control is required for the development of DW-based spintronics devices.

Acknowledgment

This work was supported in part by the National Research Foundation of Korea funded by the Ministry of Education, Science, and Technology (2011-0016497), the IT R&D Program of Ministry of Knowledge Economy (2009-F-004-01), and the KRCF-DRC Program. The work of B. S. Chun was supported by the National Research Foundation of Korea (NRF-2010-359-D00033).

REFERENCES

[1] G. Tatara, Y.-W. Zhao, M. Muñoz, and N. García, "Domain wall scattering explains 300% ballistic magnetoconductance of nanocontacts," *Phys. Rev. Lett.*, vol. 83, pp. 2030–2033, 1999.

[2] D. A. Allwood, G. Xiong, M. D. Cooke, C. C. Faulkner, D. Atkinson, N. Vernier, and R. P. Cowburn, "Submicrometer ferromagnetic NOT gate and shift register," *Science*, vol. 296, pp. 2003–2006, 2002.

[3] J.-E. Wegrowe, T. Wade, X. Hoffer, L. Gravier, J.-M. Bonard, and J.-Ph. Ansermet, "Magnetoresistance of nanocontacts with constrained magnetic domain walls," *Phys. Rev. B*, vol. 67, pp. 104418–104424, 2003.

[4] L. Berger, "Motion of a magnetic domain wall traversed by fast-rising current pulses," *J. Appl. Phys.*, vol. 71, pp. 2721–2723, 1992.

[5] H. Koo, C. Krafft, and R. D. Gomez, "Current-controlled bi-stable domain configurations in $Ni_{81}Fe_{19}$ elements: An approach to magnetic memory devices," *Appl. Phys. Lett.*, vol. 81, pp. 862–864, 2002.

[6] A. J. Zambano and W. P. Pratt, Jr., "Detecting domain-wall trapping and motion at a constriction in narrow ferromagnetic wires using perpendicular-current giant magnetoresistance," *Appl. Phys. Lett.*, vol. 85, pp. 1562–1564, 2004.

[7] P. Bruno, "Geometrically constrained magnetic wall," *Phys. Rev. Lett.*, vol. 83, pp. 2425–2428, 1999.

[8] S. D. Kim, B. S. Chun, D. K. Kim, and Y. K. Kim, "Simulation studies of domain wall width changes in various nanoconstriction shapes," *IEEE Trans. Magn.*, vol. 42, no. 10, pp. 2621–2623, Oct. 2006.

[9] C. K. Lim, T. Devolder, C. Chappert, J. Grollier, V. Cros, A. Vaures, A. Fert, and G. Faini, "Domain wall displacement induced by subnanosecond pulsed current," *Appl. Phys. Lett.*, vol. 84, pp. 2820–2822, 2004.